Analytical formula for output phase of symmetrically excited one-to-N multimode interference coupler

Amir Hosseini, David Kwong and Ray T. Chen
Microelectronic Research Center, Department of Electrical and Computer Engineering, University of Texas, Austin, TX 78758 USA (e-mail: ahoss@ece.utexas.edu; chen@ece.utexas.edu)

ABSTRACT

We derive analytical formulations for the output phase profile of symmetrically excited one-to-N multimode interference couplers. We show that the output phase increases quadratically from the middle of the MMI waveguide, which needs to be taken into account for phase-dependent applications such as optical phased arrays.
Keywords: Multimode Interference Coupler, Integrated Optics

1. INTRODUCTION

Multimode interference (MMI) based devices have been widely used in photonic integrated circuits (PICs) as compact size passive components power splitters [1], [2], 90◦ hybrid couplers [3] and mode-matching stages [4]. MMI-based active devices such as optical switches [5], [6] and phased array multiplexers [7] have been theoretically studied and experimentally demonstrated. The interest in MMI based devices stems from properties such as compact size, low power imbalance, stable power splitting ratio, low cross talk, large optical bandwidth, and high tolerance to fabrication process [2], [8], which render such devices suitable for integration in PICs with complex passive networks including power splitters and signal routing. Compared to Y-branches, MMI splitters are smaller and benefit from scalability as the number of the output ports grows.

Several studies investigated the quality of the output signals in MMI couplers based on power uniformity [3], [9] and image resolution [10]. Also, several techniques have been proposed to improve the signal quality, such as tapered multimode waveguide [11], graded-index waveguide [12] and deeply etched air trenches at the boundary of the multimode section [2]. In addition to power splitter, MMI coupler can be used in more complex photonic components where the phase of the output signal is also important, such as 90◦ hybrid couplers [3].

In addition to power splitter, MMI coupler can be used in more complex photonic components where the phase of the output signal is also important, such as 90◦ hybrid couplers [3]and in high-speed phased array optical beam steering [13]. Despite the effort in investigating the power profile at the MMI output ports, there have been no studies on the output phase profile. In many applications,

Optoelectronic Interconnects and Component Integration IX, edited by Alexei L. Glebov, Ray T. Chen,
Proc. of SPIE Vol. 7607, 760718 · © 2010 SPIE · CCC code: 0277-786X/10/$18 · doi: 10.1117/12.839906

Downloaded from SPIE Digital Library on 04 Apr 2010 to 128.83.63.21. Terms of Use: http://spiedl.org/terms

the knowledge of the phase pro file is important. The phase differences of MMI output ports can severely distort the performance of compact optoelectronic devices that employ a multimode waveguide region to generate several channels with linear phase profiles such as optical spatial quantized analog-to-digital converters [14] and GHz Optical beam steerers [15]. The knowledge of the MMI output phase profile will provide a means to apply appropriate phase shifts in order to attain the desired phase profile.

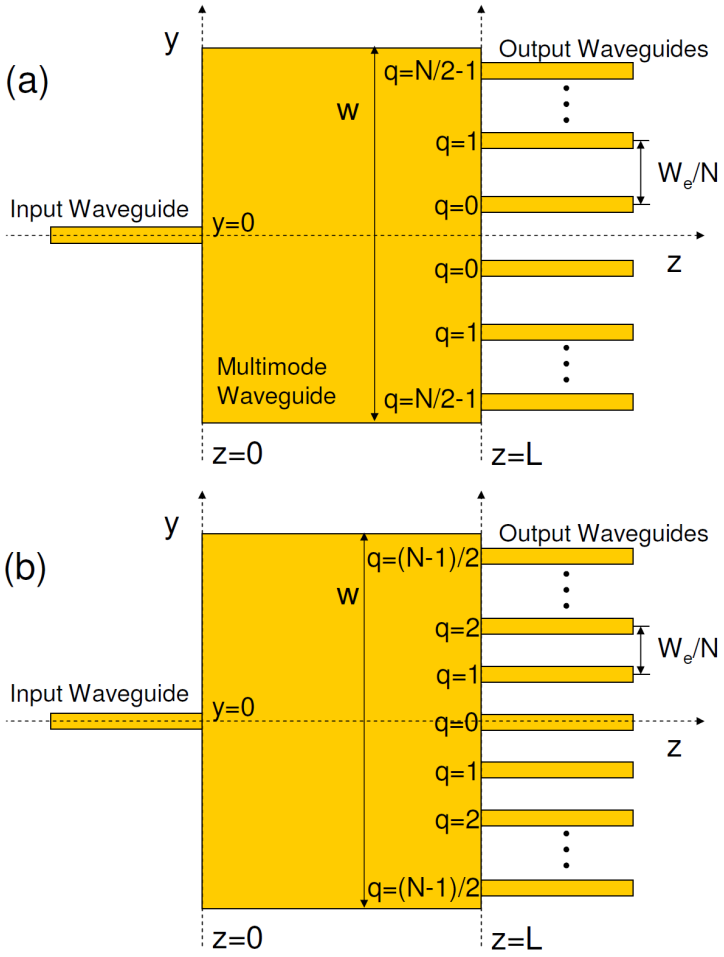

Fig. 1, Schematics of 1 × N symmetric MMI coupler, (a) even N, (b) odd N.

Symmetrically excited one-to-N MMI couplers are the most common power splitters in photonic circuitries, where the number of output ports has been reported from 2 to as large as 64 [16]. In this paper, we derive an analytical formula for the symmetrically excited MMI output phase profile, and

Downloaded from SPIE Digital Library on 04 Apr 2010 to 128.83.63.21. Terms of Use: http://spiedl.org/terms

compare the results with beam propagation simulations. Additionally, we report a complete description of the output field profile at the symmetric N-fold imaging length in ideal MMI couplers. Our analysis is most accurate for high index contrast waveguides. However, image enhancing techniques, such as etched air trenches introduced to define the edges of the MMI coupler [2], make the presented analysis applicable to low index contrast waveguides, such as polymer based structures. Such etched air trenches reduce the lateral penetration depth into the cladding so that the effective width of all the guided modes is approximately the same as the actual width of the MMI coupler, and therefore improve the output power uniformity.

2. MULTIMODE INTERFERENCE COUPLERS

Self-imaging is a phenomenon in multimode waveguides by which an input field profile is reproduced in single or multiple images at periodic intervals along the propagation direction of the guide [3]. This effect has been exploited in different MMI based structures. Several MMI coupler structures have been theoretically studied and experimentally fabricated [1]–[3], [9], [10], [16]. In Fig. 1 the multimode waveguide section consists of a W -wide core of refractive index nc, embedded in between cladding layers of n_0. In the case of 3D waveguides, an equivalent 2D representation can be made by techniques such as the effective index method or the spectral index method [3]. The multimode section can support maximum M + 1 number of modes. For each mode p, the dispersion relation is given as

$$\beta_p^2 + \kappa_{yp}^2 = \left(\frac{2\pi n_c}{\lambda_0} \right)^2, \tag{11}$$

where, β_p is the propagation constant of the the pth mode, λ_0 is a free-space wavelength. κ_{yp} is the lateral wavenumber of the pth mode, given as $\kappa_{yp} = (p+1)\pi/W_e$, where W_e is the effective width for mode m including the penetration depth due to the Goose-Hahnchen shift [2]. The propagation constant β_p can be approximated as

$$\beta_p \approx \beta_0 - \frac{p(p-2)}{3L_\pi}, \tag{12}$$

where, $L_\pi = \pi/(\beta_0 - \beta_1) \approx 4n_c W_e^2/3\lambda_0$. Given the orthogonality of the propagating modes, any input field profile at z = 0, can be written as a linear combination of the propagating modes,

Downloaded from SPIE Digital Library on 04 Apr 2010 to 128.83.63.21. Terms of Use: http://spiedl.org/terms

$$\Phi(y, z=0) = \sum_{p=0}^{M} c_p \phi_p(y), \tag{13}$$

where cp is the excitation coefficient of the pth mode by the given input field profile, calculated as the overlap integrals of the pth mode and the input field profile [3]. Each excited mode accumulates phase shift according to its propagation constants and therefore, the field profile at any z = L can be represented by

$$\exp(-j\beta_0 L)\sum_{p=0}^{M} c_p \phi_p(y) \exp\left(-j(\beta_p - \beta_0)L\right) \approx$$
$$\exp(-j\beta_0 L)\sum_{p=0}^{M} c_p \phi_p(y) \exp\left(j\frac{p(p+2)\pi}{3L_\pi}L\right). \tag{14}$$

At L =3rL$_\pi$ with r =1, 2, ..., all the exponential terms in (4) becomes in-phase with one another and a single image of the input field profile is formed. Generally, an N-fold image of the input field profile is formed At L =3L$_\pi$/N. In the case of symmetric excitation, Φ(y,Z =0) =Φ(y,Z =0), only the even modes p =2m, for integer m, are excited. This type of excitation can be realized by a symmetric input filed profile fed to the center of the multimode waveguide Fig. 1. This has been known to result in short 1xN couplers, where N is the number of output ports [3]. The required length for such a coupler is given as which is four times shorter than the general case. L =3rL$_\pi$/4N, r integer.

In the case of 1xN couplers, the output power is ideally designed to be equally divided among the output ports and therefore, the field amplitude at the output ports is 1/√N. In reality, however, the approximation in (2) becomes inaccurate especially for the higher order modes in low refractive index contrast waveguides. In these cases, the Goose-Hahnchen effect becomes mode dependent and the accumulated phase shift of each mode is different from the ideal case by an error of

$$\Delta\varphi_p \approx \frac{\lambda_0^2 (p+1)^4 \pi}{2Nn_c^2 W_{eff}^2}\left[1/8 - \frac{\lambda_0 n_c^2}{6\pi W_w (n_c^2 - n_0^2)^{1.5}}\right] \tag{15}$$

for the N-fold imaging length L =3rL$_\pi$/N [9]. The existence of these modal phase errors is inherent in the dispersion law of the dielectric slab waveguides. Additional phase errors happen when the observation plane is shifted away from the paraxial plane [10]. In the case of the symmetric excitation, the accumulated phase error at the N-fold imaging length is $\Delta\psi_p/4$. This error would result in non-uniformity in the output power distribution. The phase profile of the output ports and the effect of non-ideal effects on the output phase profile have not been investigated. In the next

Downloaded from SPIE Digital Library on 04 Apr 2010 to 128.83.63.21. Terms of Use: http://spiedl.org/terms

section we derive a closed form formula for the output field profile.

3. SYMMETRIC MMI COUPLER PHASE PROFILE

Consider the 1xN MMI coupler shown in Fig. 1. In order to analyze the output properties, such as image resolution, contrast, etc, Ulrich and Kamiya approximated the multimode waveguide propagating modes field profiles with cosine functions,

$$\phi_p(y) = \cos(\kappa_{yp} y), \tag{16}$$

which allowed them to apply the Fourier transform properties to the field presentation in [10]. In this paper we adopt the same technique to take the position (in the y-direction) of the images formed into account.

Consider one of the N images of the input field at an N-fold imaging length and shifted in the y-direction to y = yq. Based on (3), this image can be presented as $B\Phi(y\text{-}y_q,\ z=0)$ $B\Phi(y-y_p, z=0) = B\sum_{p=0}^{M} c_p \varphi_p(y-y_q)$, where $B = \frac{\exp(j\theta_q)}{\sqrt{N}}$, assuming uniform power distribution.

As shown in Figs. 1(a) and (b) for the N images formed at the output ports the lateral shifts of the position with respect to the input image are yq =±We/2N, ±3We/2N..., ± (N-1)We/2N for even N, and yq =0, ±We/N, ±2We/N, ±(N-1)We/2N for odd N. Therefore, at an N-fold imaging length (L_0) the field profile $\Phi(y,L_0)$ is

$$\frac{1}{\sqrt{N}} \sum_{q=0}^{N/2-1} \exp(j\theta_q) \sum_{p=0}^{M} c_p \left(\cos\left[\kappa_{yp} (y - \frac{(2q+1)W_e}{2N}) \right] + \cos\left[\kappa_{yp} (y + \frac{(2q+1)W_e}{2N}) \right] \right), \tag{17}$$

for even N, and

$$\frac{1}{\sqrt{N}} \exp(j\theta_0) + \frac{1}{\sqrt{N}} \sum_{q=1}^{(N-1)/2} \exp(j\theta_q) \times \sum_{p=0}^{M} c_p \left(\cos\left[\kappa_{yp} (y - \frac{qW_e}{N}) \right] + \cos\left[\kappa_{yp} (y + \frac{qW_e}{N}) \right] \right), \tag{18}$$

for odd N. In (7) and (8), the symmetry of the structure have been taken into account by letting $\theta_{-q} = \theta_q$. We can simplify (7) and (8) using the trigonometric identity cos(a+b)= cos(a)cos(b)-sin(a)sin(b). We also note that when the multimode waveguide is symmetrically excited, only the even modes of

Downloaded from SPIE Digital Library on 04 Apr 2010 to 128.83.63.21. Terms of Use: http://spiedl.org/terms

the multimode region are excited, and therefore c_p =0 for odd p values. We can rewrite (7) and (8) with $c_p = c_{2m}$

$$\frac{2}{\sqrt{N}} \sum_{q=0}^{N/2-1} \exp(j\theta_q) \times \sum_{=0}^{M} c_{2m} \cos(\kappa_{yp} y) \cos\left[\frac{(2m+1)(2q+1)}{2N}\pi\right], \tag{19}$$

for even N, and

$$\frac{1}{\sqrt{N}}\exp(j\theta_0) + \frac{2}{\sqrt{N}} \sum_{q=1}^{(N-1)/2} \exp(j\theta_q) \times \sum_{m=0}^{M/2} c_{2m} \cos(\kappa_{yp} y) \cos\left[\frac{(2m+1)q}{N}\pi\right], \tag{20}$$

for odd N. We can also rewrite the field profile from (4) at a symmetric N-fold imaging length, L_0 =$3L_\pi/4N$, considering p =2m

$$\Phi(y, L_0) = \sum_{m=0}^{M/2} c_{2m}\phi_{2m}(y)\exp(j\frac{m(m+1)}{N}\pi). \tag{21}$$

Note that we have dropped the common factor $\exp(-j\beta_0 L_0)$, for simplicity, but we will add it back later. Using the reciprocity law for quadratic Gauss sums we can show that in the case of even N

$$\sum_{m=0}^{M/2} C_{2m}\phi_{2m}(y)\exp\left[j\frac{m(m+1)}{N}\pi\right] = \frac{2\exp(j\frac{N-2}{4N}\pi)}{\sqrt{N}} \sum_{m=0}^{M/2} C_{2m}\phi_{2m}(y) \times \sum_{q=0}^{N/2-1} \exp\left(-j\frac{q(q+1)}{N}\pi\right)\cos\left(\frac{(2m+1)(2q+1)\pi}{2N}\right). \tag{22}$$

Comparing (12) and (9), one can conclude that

$$\exp(j\theta_q) = \exp(j\frac{N-2}{4N}\pi) \times \exp(-j\frac{q(q+1)}{N}\pi). \tag{23}$$

Taking in the common factor, $\exp(-j\beta_0 L_0)$, into account,

$$\theta_q = -\beta_0 L_0 + \frac{N-2-4q(q+1)}{4N}\pi, \tag{24}$$

for q = 0, 1..., N/2-1, where q is assigned to the output ports as shown in Fig. 1(a). Note that the

Downloaded from SPIE Digital Library on 04 Apr 2010 to 128.83.63.21. Terms of Use: http://spiedl.org/terms

phase profile is symmetric with respect to the line y = 0.We can identify that the phase profile has a propagation accumulated phase term, a constant term depending on the number of output channels, which is the same for all the channels, and a term that quadratically depends on the channel number (starting from the middle of the waveguide). In the case of odd N, one can show

$$\sum_{m=0}^{M/2} C_{2m}\phi_{2m}(y)\exp\left[j\frac{m(m+1)}{N}\pi\right] = \frac{\exp(j\frac{N-1}{4N}\pi)}{\sqrt{N}}\sum_{m=0}^{M/2} C_{2m}\phi_{2m}(y)\times \left(1+2\sum_{q=1}^{(N-1)/2}\exp\left(-j\frac{q^2}{N}\pi\right)\cos\left(\frac{(2m+1)q\pi}{N}\right)\right). \quad (25)$$

Similarly, in the case of odd N, comparing (15) and (10) one can conclude that

$$\theta_q = -\beta_0 L_0 + \frac{N-1-4q^2}{4N}\pi, \quad (26)$$

for q = 0, 1, ...(N - 1)/2, where the q values are assigned to the output ports as shown in Fig. 1(b). Again, the phase profile is symmetric with respect to the line y = 0. Although the discussion in this paper is based on dielectric waveguides, similar results are expected in the case of self-imaging in other waveguiding structures, such as multimode photonic crystal waveguides, which can be realized by removing several periods in the transverse direction [17].

Appendix I: Proof for even N

In the case of $N = 2K$ and $K \in Z$, we need to show

$$\sum_{m=0}^{M/2} C_{2m}\phi_{2m}(y)\exp\left[j\frac{m(m+1)}{N}\pi\right] = \frac{2\exp(j\frac{N-2}{4N}\pi)}{\sqrt{N}}\sum_{m=0}^{M/2} C_{2m}\phi_{2m}(y)\times\sum_{q=0}^{N/2-1}\exp\left(-j\frac{q(q+1)}{N}\pi\right)\cos\left(\frac{(2m+1)(2q+1)\pi}{2N}\right). \quad (17)$$

Note that y in (17) is an independent variable. Therefore, in order to prove (17), we need to show that for every m, the coefficients of $C_{2m}\varphi_m(y)$ on the left and right sides of (17) are equal. Thus, we need to prove

Downloaded from SPIE Digital Library on 04 Apr 2010 to 128.83.63.21. Terms of Use: http://spiedl.org/terms

$$\exp\left[j\frac{m(m+1)}{N}\pi \right] = \frac{2\exp(j\frac{N-2}{4N}\pi)}{\sqrt{N}} \times \sum_{q=0}^{N/2-1} \exp\left(-j\frac{q(q+1)}{N}\pi \right) \cos\left(\frac{(2m+1)(2q+1)\pi}{2N} \right), \tag{18}$$

which simplifies to

$$\frac{2\exp(j\frac{N-2}{4N}\pi)}{\sqrt{2K}} \sum_{q=0}^{K-1} \exp\left(-j\frac{q(q+1)+m(m+1)}{2K}\pi \right) \cos\left(\frac{(2m+1)(2q+1)\pi}{4K} \right) = 1 \tag{19}$$

Let us simplify the left hand side of (19):

$$\frac{2\exp(j\frac{K-1}{4K}\pi)}{\sqrt{2K}} \times \{ \sum_{q=0}^{K-1} \exp\left(-j\frac{2q(q+1)+2m(m+1)-(2m+1)(2q+1)}{4K}\pi \right) \exp\left(-j\frac{2q(q+1)+2m(m+1)+(2m+1)(2q+1)}{4K}\pi \right) \} = 1 \tag{20}$$

which further simplifies to

$$\frac{2\exp(j\frac{1}{4}\pi)}{\sqrt{2K}} \sum_{q=0}^{K-1} \{ \exp\left(-j\frac{(m-q)^2}{2K}\pi \right) + \exp\left(-j\frac{(m+q+1)^2}{2K}\pi \right) \}. \tag{21}$$

Now note that

$$\sum_{q=0}^{K-1} \{ \exp\left(-j\frac{(m-q)^2}{2K}\pi \right) + \exp\left(-j\frac{(m+q+1)^2}{2K}\pi \right) \} = \sum_{q=m+1-K}^{m+K} \exp\left(-j\frac{q^2}{2K}\pi \right). \tag{22}$$

Consider a set of integer numbers {m-K+1, m-K+2…,m+K}. Regardless of m, this set imodules 2K is exactly the same as {0, 1…,2K-1}mod(2K). it can be easily shown that if $a \equiv b \bmod(2K)$, then $a^2 \equiv b^2 \bmod(4K)$, hence $\exp(-j2\pi a^2/4K) = \exp(-j2\pi b^2/4K)$ or $\exp(-j2\pi a^2/4K) = \exp(-j2\pi b^2/K)$. Therefore, the expression in (22) is independent of m as follows,

$$\sum_{q=m+1-K}^{m+K} \exp\left(-j\frac{q^2}{2K}\pi \right) = \sum_{q=0}^{2K-1} \exp\left(-j\frac{q^2}{2K}\pi \right). \tag{23}$$

From the abovementioned statements we can also conclude

$$\sum_{q=0}^{2K-1} \exp\left(-j\frac{q^2}{2K}\pi \right) = \sum_{q=1}^{2K} \exp\left(-j\frac{q^2}{2K}\pi \right) = \sum_{q=2K+1}^{4K} \exp\left(-j\frac{q^2}{2K}\pi \right), \tag{24}$$

which leads to

Downloaded from SPIE Digital Library on 04 Apr 2010 to 128.83.63.21. Terms of Use: http://spiedl.org/terms

$$\sum_{q=m+1-K}^{m+K} \exp\left(-j\frac{q^2}{2K}\pi\right) = \frac{1}{2}\sum_{q=1}^{4K} \exp\left(-j\frac{q^2}{2K}\pi\right). \tag{25}$$

Using the reciprocity law for quadratic Gauss sums defined as

$$G(N;M) = \sum_{q=1}^{M} \exp(j2\pi Nq^2/M), \tag{26}$$

we can write the results as follows

$$G(N=1;M) = \sum_{q=1}^{M} \exp(j2\pi q^2/M) = \frac{1}{2}\sqrt{M}(1+j)[1+\exp(-j\pi M/2)], \tag{27}$$

which is equal to $(1+j)\sqrt{M}$ if $M \equiv 0 \bmod(4)$. Comparing (25) and (27) we can conclude that

$$\begin{aligned}&\sum_{q=m+1-K}^{m+K} \exp\left(-j\frac{q^2}{2K}\pi\right) = \frac{1}{2}G^*(1,4K) = \\ &\frac{1}{2}(1-j)\sqrt{4K} = (1-j)\sqrt{K} = \exp(-j\frac{\pi}{4})\sqrt{2K},\end{aligned} \tag{28}$$

where, G* is the complex conjugate of G. Consider (19), (22), (23) and (28), we can write

$$\begin{aligned}&\frac{2\exp(j\frac{N-2}{4N}\pi)}{\sqrt{2K}}\sum_{q=0}^{K-1}\exp\left(-j\frac{q(q+1)+m(m+1)}{2K}\pi\right)\cos\left(\frac{(2m+1)(2q+1)\pi}{4K}\right) = \\ &\frac{e^{j\pi/4}}{\sqrt{2K}}\sum_{q=0}^{2K-1}\exp(-j\frac{q^2}{2K}\pi) = \frac{e^{j\pi/4}}{\sqrt{2K}}\times\exp(-j\frac{\pi}{4})\sqrt{2K} = 1.\end{aligned}$$

Therefore, we have proved (18) and consequently (17).

Appendix II: Proof for odd N

In the case of $N = 2K+1$ and $K \in Z$, we need to show

$$\begin{aligned}&\sum_{m=0}^{M/2} C_{2m}\phi_{2m}(y)\exp\left[j\frac{m(m+1)}{N}\pi\right] = \\ &\frac{\exp(j\frac{N-1}{4N}\pi)}{\sqrt{N}}\sum_{m=0}^{M/2} C_{2m}\phi_{2m}(y)\times\left(1+2\sum_{q=1}^{(N-1)/2}\exp\left(-j\frac{q^2}{N}\pi\right)\cos\left(\frac{(2m+1)q\pi}{N}\right)\right).\end{aligned} \tag{29}$$

Downloaded from SPIE Digital Library on 04 Apr 2010 to 128.83.63.21. Terms of Use: http://spiedl.org/terms

Similar to the case of even N, since y in (17) is an independent variable, in order to prove (29), we need to show that for every m, the coefficients of $C_{2m}\varphi_m(y)$ on the left and right sides of (29) are equal. Thus, we need to prove

$$\exp\left[j\frac{m(m+1)}{N}\pi \right] = \frac{\exp(j\frac{N-1}{4N}\pi)}{\sqrt{N}}\left(1+2\sum_{q=1}^{(N-1)/2}\exp\left(-j\frac{q^2}{N}\pi\right)\cos\left(\frac{(2m+1)q\pi}{N}\right)\right), \tag{30}$$

or equivalently,

$$\frac{\exp(j\frac{2K}{4(2K+1)}\pi)}{\sqrt{2K+1}}\{\exp\left[-j\frac{m(m+1)}{2K+1}\pi\right]+ 2\sum_{q=1}^{K}\exp\left(-j\frac{q^2+m(m+1)}{2K+1}\pi\right)\cos\left(\frac{(2m+1)q\pi}{2K+1}\right)\}=1, \tag{31}$$

Consider the left-side of (31)

$$\frac{\exp(j\frac{2K}{4(2K+1)}\pi)}{\sqrt{2K+1}}\{\exp\left[-j\frac{m(m+1)}{2K+1}\pi\right]+ \sum_{q=1}^{K}\exp\left(-j\frac{q^2+m(m+1)-(2m+1)q}{2K+1}\pi\right)+\exp\left(-j\frac{q^2+m(m+1)+(2m+1)q}{2K+1}\pi\right)\}, \tag{32}$$

which simplifies to

$$\frac{\exp(j\frac{2K}{4(2K+1)}\pi)}{\sqrt{2K+1}}\{\exp\left[-j\frac{m(m+1)}{2K+1}\pi\right]+ \sum_{q=1}^{K}\exp\left(-j\frac{(q-m-1/2)^2-1/4}{2K+1}\pi\right)+\exp\left(-j\frac{(q+m+1/2)^2-1/4}{2K+1}\pi\right)\}, \tag{33}$$

and further simplies to

$$\frac{\exp(j\frac{1}{4}\pi)}{\sqrt{2K+1}}\{\exp\left[-j\frac{(m+1/2)^2}{2K+1}\pi\right]+ \sum_{q=1}^{K}\exp\left(-j\frac{(q-m-1/2)^2}{2K+1}\pi\right)+\exp\left(-j\frac{(q+m+1/2)^2}{2K+1}\pi\right)\}. \tag{34}$$

Note that

Downloaded from SPIE Digital Library on 04 Apr 2010 to 128.83.63.21. Terms of Use: http://spiedl.org/terms

$$\exp\left[-j\frac{(m+1/2)^2}{2K+1}\pi\right]+\sum_{q=1}^{K}\{\exp\left(-j\frac{(q-m-1/2)^2}{2K+1}\pi\right)+$$
$$\exp\left(-j\frac{(q+m+1/2)^2}{2K+1}\pi\right)\}=\sum_{q=-K}^{K}\exp\left(-j\frac{(2q+2m+1)^2}{4(2K+1)}\pi\right). \quad (35)$$

Consier $q=n(2K+1)+r$, $-K\le q\le K$ and $0\le r\le 2K$. Then, $\{q+m\}\bmod(2K+1)\equiv\{q\}\bmod(2K+1)$ with the same set of residuals {r}, for every integer m. In addition, $\{2q+2m+1\}\bmod(2K+1)$ is the set of {2r+1}. Therefore, $\forall m\in Z$ and $\forall q\in\{q\}$, $\exists r\in\{q\}$ so that 2m+2q+1=2p(2K+1)+(2r+1) for some integer p. Thus, we can write

$$(2m+2q+1)^2=4p(2K+1)[p(2K+1)+(2r+1)]+(2r+1)^2 \quad (36)$$

Also not that p[p(2K+1)+(2r+1)] is always ever. Thus, $(2m+2q+1)^2=8s(2K+1)+(2r+1)^2$ for some interger s. and

$$\sum_{q=-K}^{K}\exp\left(-j\frac{(2q+2m+1)^2}{4(2K+1)}\pi\right)=\sum_{r=0}^{2K}\exp\left(-j\frac{(2r+1)^2}{4(2K+1)}\pi\right)=$$
$$\exp\frac{-j\pi}{2(2K+1)}\sum_{r=0}^{2K}\exp\frac{r^2+r}{2K+1}\pi. \quad (37)$$

Now consider the Gauss Quadratic Reciprocity law $\forall a,b,c,z\in Z$, $ac\neq 0$ and even $ac+b$

$$\sum_{z=0}^{|c|-1}\exp\left(j\pi\frac{az^2+bz}{c}\right)=\sqrt{|c/a|}\exp\left(j\pi\frac{|ac|-b^2}{4ac}\right)\sum_{z=0}^{|a|-1}\exp\left(j\pi\frac{cz^2+bz}{a}\right). \quad (38)$$

Let $a,b=1$, $z=r$ and $c=2K+1$, we can say $ac+b=2K+2$ is always even, therefore, we can use the Gauss Quadratic Reciprocity law as follows

$$\exp\frac{-j\pi}{2(2K+1)}\sum_{r=0}^{2K}\exp\frac{r^2+r}{2K+1}\pi.=$$
$$\exp\frac{-j\pi}{2(2K+1)}\times\sqrt{2K+1}\exp\left(-j\pi\frac{2K}{4(2K+1)}\right)=\sqrt{2K+1}\exp(-\frac{\pi}{4}). \quad (39)$$

From (34) and (39) we conclude

$$\frac{\exp(j\frac{1}{4}\pi)}{\sqrt{2K+1}}\{\exp\left[-j\frac{(m+1/2)^2}{2K+1}\pi\right]+$$
$$\sum_{q=1}^{K}\exp\left(-j\frac{(q-m-1/2)^2}{2K+1}\pi\right)+\exp\left(-j\frac{(q+m+1/2)^2}{2K+1}\pi\right)\}= \quad (40)$$
$$\frac{\exp(j\frac{1}{4}\pi)}{\sqrt{2K+1}}\times\sqrt{2K+1}\exp(-j\frac{1}{4}\pi)=1$$

Therefore, we have proved (30) and consequently (29).

Downloaded from SPIE Digital Library on 04 Apr 2010 to 128.83.63.21. Terms of Use: http://spiedl.org/terms

REFERENCES

[1] J. S. Yu, J. Y. Moon, S. M. Choi, and Y. T. Lee, "Fabrication of 1x8multimode-interference optical power splitter based on inp using ch4/h2 reactive ion etching," Japanese Journal of Applied Physics 40, 634–639 (2001).

[2] X. Wang and R. T. Chen, "Image enhanced polymer-based multimode interference coupler covering c and l bands using deeply etched air trenches," Applied Physics Letters 90(11), 111106 (2007).

[3] L. Soldano and E. Pennings, "Optical multi-mode interference devices based on self-imaging: principles and applications," J. Lightwave Technology 13(4), 615–627 (1995).

[4] X. Chen, W. Jiang, J. Chen, L. Gu, and R. T. Chen, "20 db-enhanced coupling to slot photonic crystal waveguide using multimode interference coupler," Applied Physics Letters 91(9), 091111 (2007).

[5] Y.-J. Chang, T. K. Gaylord, and G.-K. Chang, "Pulse response of multimode interference devices," J. Lightwave Technology 24(3), 1462 (2006).

[6] J. Xia, J. Yu, Z. Wang, Z. Fan, and S. Chen, "Low power 22 thermooptic soi waveguide switch fabricated by anisotropy chemical etching," Optics Communications 232, 223–228 (2004).

[7] M. Paiam and R. MacDonald, "A 12-channel phased-array wavelength multiplexer with multimode interference couplers," IEEE Photonics Technology Letters 10(2), 241–243 (1998).

[8] M. Rajarajan, B.Rahman, T. Wongcharoen, and K. Grattan, "Accurate analysis of MMI devices with two-dimensional confinement," J. Lightwave Technology 14(9), 2078–2084 (1996).

[9] J. Huang, R. Scarmozzino, and J. Osgood, R.M., "A new design approach to large input/output number multimode interference couple rsand its application to low-crosstalk WMD routers," IEEE Photonics Technology Letters 10(9), 1292–1294 (1998).

[10] R. Ulrich and T. Kamiya, "Resolution of self-images in planar optical waveguides," J. Optical Society of America 68(5), 583–592 (1978).

[11] R.M.Lorenzo, C. Llorente, and E. J. A. M. Lopez, "Improved self-imaging characteristics in i x n multimode couplers," Proc. of IEE Oproelectron 145(1), 65–69 (1998).

[12] R. Yin, X. Jiang, J. Yang, and M. Wang, "Structure with improved self imaging in its graded-index multimode interference region," J. Optical Society of America B 19(6), 1301–1303 (2002).

[13] M. Jarrahi, R. F. W. Pease, D. A. B. Miller, and T. H. Lee, "Optical switching based on high-speed phased array optical beam steering," Applied Physics Letters 92(1), 014106 (2008).

[14] M. Jarrahi, R. F. W. Pease, and T. H. Lee, "Spatial quantized analog-to-digital conversion based on optical beam-steering," J. Lightwave Technology 26(14), 2219–2226 (2008).

[15] R. F. P. M. Jarrahi, D. A. Miller, and T. H. Lee, "An overview of optical phased array technology and status," Applied Physics Letters 92, 014106 (2008).

[16] T. Rasmussen, J. Rasmussen, and J. Povlsen, "Design and performance evaluation of 1-by-64 multimode interference power splitter for optical communications," J. Lightwave Technology 13(10), 2069–2074 (1995).

[17] Z. Li, Y. Zhang, and B. Li, "Terahertz photonic crystal switch in silicon based on self-imaging principle," Optics Express 14(9), 3887–3892 (2006).

Downloaded from SPIE Digital Library on 04 Apr 2010 to 128.83.63.21. Terms of Use: http://spiedl.org/terms